THESIS FOR THE DEGREE OF LICENTIATE OF ENGINEERING IN MACHINE AND VEHICLE SYSTEMS

On Tyre Rotation Modelling and Cooling Flow Measurements

TEDDY HOBEIKA

Department of Applied Mechanics
Division of Vehicle Engineering and Autonomous Systems
CHALMERS UNIVERSITY OF TECHNOLOGY

Göteborg, Sweden 2015

On Tyre Rotation Modelling and Cooling Flow Measurements
TEDDY HOBEIKA

Thesis for the degree of Licentiate of Engineering 2015:15
ISSN 1652-8565
Department of Applied Mechanics
Division of Vehicle Engineering and Autonomous Systems
Chalmers University of Technology
SE-412 96 Göteborg
Sweden
Telephone: +46 (0)31-772 1000

Chalmers Reproservice
Göteborg, Sweden 2015

On Tyre Rotation Modelling and Cooling Flow Measurements
Thesis for the degree of Licentiate of Engineering in Machine and Vehicle Systems
TEDDY HOBEIKA
Department of Applied Mechanics
Division of Vehicle Engineering and Autonomous Systems
Chalmers University of Technology

Abstract

With the technological computer advancements, vehicle development is relying more and more on simulations as an alternative to testing. A similar trend follows in aerodynamic development of vehicles where Computational Fluid Dynamics(CFD) simulations are increasing in complexity and accuracy. Even though these simulations have previously been used to evaluate trends of different design and analyse the flow field around the car, they are aimed at being used to predict exact figures in the future.

Wheel flow aerodynamics has been the focus of CFD research for several years now especially with the expected introduction of the WLTP regulations, which will require car manufactures to evaluate the drag of the vehicle for all different rim and tyre combinations the car could have in order to determine its official fuel consumption. Thus correct and accurate modelling of tyre and rims in CFD is a high priority for vehicle manufacturers in order optimize vehicle design without large increases in testing costs. This thesis investigates the effects of different wheel geometries as well as different wheel rotation modelling techniques and their effect on overall vehicle forces.

An important parameter to consider when validating simulations is the cooling flow as the amount of air going through the vehicles engine bay changes the airflow around the car thus affecting the flow directed towards the wheels. In this thesis a novel, simple, and quick method for measuring cooling flow is introduced. This allows the monitoring of cooling flow during aerodynamic development at low costs especially with the introduction of grill shutters as a further step to reduce aerodynamic drag when cooling flow is not needed.

Keywords: CFD, Aerodynamics, Tyres, cooling flow, air mass flow

To all the training hours I have missed for this work

Acknowledgements

I would like to thank Tim Walker and Dr. Christoffer Landström for their guidance and support with all tests and aerodynamics discussions during the time I spent at Volvo Cars. A special thanks to Dr. Peter Gullberg for his enlightening discussions and help with the fan test rig at Volvo GTT, as without his help those tests would not be possible. I would also like to thank Dr. Simone Sebben for her constant support and guidance through my PhD project as well as direct advice on CFD simulations. A big thanks to Prof. Lennart Löfdahl without whom this whole work would not be possible. And last but not least, a big thanks to my steering committee and the Swedish Energy Agency for providing funding and support for my PhD project.

Thesis

This thesis consists of an extended summary and the following appended papers:

Paper A	T. Hobeika, S. Sebben, and C. Landstrom. Investigation of the Influence of Tyre Geometry on the Aerodynamics of Passenger Cars. *SAE Int. J. Passeng. Cars - Mech. Syst.* 6 (1 2013), pp. 316–325. ISSN: 1946-4002. DOI: 10.4271/2013-01-0955
Paper B	T. Hobeika, S. Sebben, and L. Lofdahl. "Study of Different Tyre Simulation Methods and Effects on Passenger Car Aerodynamics". *International Vehicle Aerodynamics Conference 2014*. Holywell Park, Loughborough, UK, 2014, pp. 187–195. ISBN: 978-0-08-100199-8
Paper C	T. Hobeika, S. Sebben, and L. Lofdahl. A Novel Approach for Air Flow Rate Measurement Through Heat Exchangers. *Experiments in Fluids* (2015). submitted

Other publications related to thesis

Publication I	T. Hobeika, A. Vdovin, and L. Lofdahl. "Influence of Rims and Tyres on the Aerodynamic Resistance of Passenger Vehicles". *Tagung Fahrzeugaerodynamik*. Munich, Germany, 2014

Contents

Part I
Extended Summary

1 Introduction

1.1 Background Information

The drive for reduced fuel consumption and CO2 emissions requires engineers in the automotive industry to push the boundaries of their designs. To achieve more efficient systems, all possible improvement areas are exploited. One area where potential is still thoroughly investigated is aerodynamics, as regardless whether the powertrain is electric or combustion, air resistance is and will always be present.
With the introduction of the Worldwide harmonized Light vehicles Test Procedures (WLTP) regulations, aerodynamics is given a higher impact as the average speed of the test cycle rises compared to the New European Driving Cycle (NEDC). Furthermore validation of the aerodynamic drag of the vehicles will be performed for a variety of car configurations and not only a baseline configuration chosen by the vehicle manufacturer. This also includes the different tyre and rim configurations that the customer could order on the car. This adds additional challenges for the aerodynamic design of the vehicle since optimizing the vehicle for different tyre and rim configurations through wind tunnel tests becomes quite expensive, as the testing time rises significantly. As an alternative, vehicle manufacturers look at Computational Fluid Dynamics (CFD) simulations to be able to analyze these effects without the need for additional testing time. This is a quite natural move as most of the vehicle design process has been pushed more and more into simulations over the past decade, due to both cost cuts as well as increased accuracy and confidence in simulation results. With that being said research on tyre and rim designs have been an interesting area for aerodynamicists for a couple decades with papers on wheel aerodynamics dating back to the 70's, 80's and 90's [1–9], long before the WLTP regulations came along. However one must acknowledge that the research on the topic has been on the rise and can be seen in [10–20], which focused on rim designs, general wheel aerodynamics, and/or the wheel's interaction with the vehicle. Also an increase in research on tyre aerodynamics has been clear [21–26] with focus on the tyre geometry, tyre modelling techniques, and the tyre's aerodynamic effect on the rest of the vehicle.
An alternative method currently used by vehicle manufactures to reduce drag are grill shutters. Grill shutters are used when the air going through the car's cooling system exceeds the cooling requirements. At this point a grill shutter can be engaged in order to block part of the grill intake and limit the airflow through the engine bay, thus reducing cooling flow and reducing the vehicle's overall drag. Also optimization of such a system does not vary a lot from the normal optimization routines for cooling flow where knowledge of the mass flow through the radiator is essential. With a general push in industry to increase system efficiencies and push optimization limits, rises the need for fast, accurate and cheap methods to evaluate systems.

Traditional approaches rely on measuring fluid properties such as pressure or velocity. Pressure measurements are achieved using pressure probes. This requires two pressure measurements. If two static pressures are measured then a pressure drop across the core can be calculated. If one total and one static pressure are measured then the dynamic pressure can be calculated. Both methods allow for the measurement of the velocity over that point. Some different setups utilizing this method in application can be seen in many works [27–29]. Velocity measurements are achieved using anemometers. This can be achieved using hot wires where the cooling rate of the wire indicates the air flow velocity. It can also be simply achieved by placing small propellers in the air flow and the speed of the propeller rotation indicates the velocity of the air. Some different setups utilizing this method in application can be seen in many works [27, 30, 31]. These methods usually result in a measurement of the average velocity over a certain area, yet there usually still exist gaps between the measurement samples which require interpolations or assumptions. A combination of pressure and velocity measurements is also performed by Williams [32]. The traditional approaches require multiple measurements to be performed at many local points around the radiator core. With an increase in measurement points comes not only an increase in accuracy but also an increase in equipment blockage, which alters the flow, as well as an increase in measurement equipment demand. Also going from these local measurements to the global mass flow, introduces additional interpolation and discretization uncertainties.

This paper presents a novel approach to quantify the air flow through the radiator core globally without the need for multiple local measurements. The approach relies on measuring the physical effects of the fluid on the solid; thus looking at the resultant force acting on the radiator core. From the force, the air mass flow is calculated. To demonstrate the method, it has been applied on a radiator mounted in a complex flow field environment, a vehicle. Testing the radiator in a vehicle represents one of the most common applications of radiators. Along with this new method, a more traditional pressure-based measurement for quantifying mass flow is also performed for comparison purposes.

1.2 Objective

This work is part of a larger project looking mainly at tyre aerodynamics and cooling flow, as well as the interaction between the two. As it is quite known in todays engineering world, simulations and experiment go hand in hand throughout the design phases, thus both the numerical and experimental aspects need to be addressed, with the numerical aspects being the main tool of development in the early project phases. The first step in tyre aerodynamics has been to investigate the different effects tyre geometry has on a vehicle and different methods of modeling the tyre rotation in CFD. On the subject of cooling flow, the experimental aspect has been the main focus to develop an accurate method for cooling flow measurements which can be easily implemented and performed in future tests.

2 Methodology

For this part of the project, the experimental and numerical works focused on different areas of the car. The the numerical work aimed at understanding the effects of modelling wheels in CFD while the experimental work aimed at quantifying the air mass flow through the radiator in a quick and cheap method.

2.1 Numerical setup

Two different simulation setups have been performed as they aimed at evaluating different things, however both simulation sets shared a common setup grounds. Both simulations where performed on a Volvo S60 model with all the geometry being cleaned and prepared using ANSA, while Harpoon has been the main mesh generator to build the volume mesh. All simulations have been solved in Fluent using k-epsilon turbulence model and standard wall-functions and finally post processing of all results is performed in Ensight.
The first set of simulations aimed at identifying the effects of different tyre features on the overall vehicle forces acting on the car when different rims are used. For that purpose an S60 production model is used with fully detailed underhood and a refined mesh around the wheels and tyres, with the tyres refined down to 1 mm and the rims down to to 2.5 mm. A slow expansion of the mesh into the volume is used to be able to better capture the flow field around the tyre pattern details. The sample of the volume mesh and refinement around the tyre can be seen in fig. 2.1.

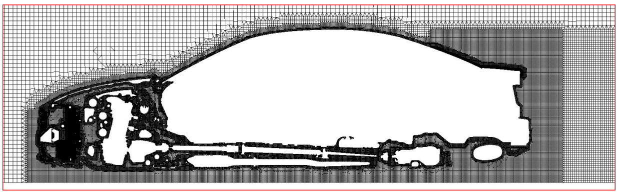

(a) *Mesh clip at symmetry plane*

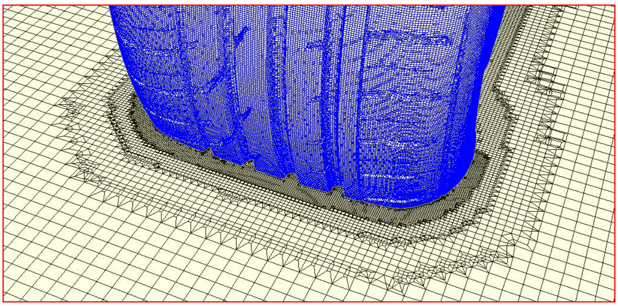

(b) *Mesh clip plane at the tyre also showing surface mesh*

Figure 2.1: *Mesh visualizations showing refinements in the volume at the vehicle centerline and the tyres*

The rims are simulated using Moving Reference Frame (MRF) approach as to limit the computational expense of the method and to be able to cover a wider range of tyre details. This naturally implies that the rim spokes' position has an effect on the results and thus a configuration with a rotated rim (Creon Rotated) is also investigated where the rim spokes are rotated so the spokes are in the opposite position.
Three different tyre pattern features have been investigated separately on four different rim designs. Also combinations of the different features have been investigated resulting in a total of 32 different configurations. The three different tyre features are shown separately in fig. 2.2 and the four rim designs are shown in fig. 2.3.

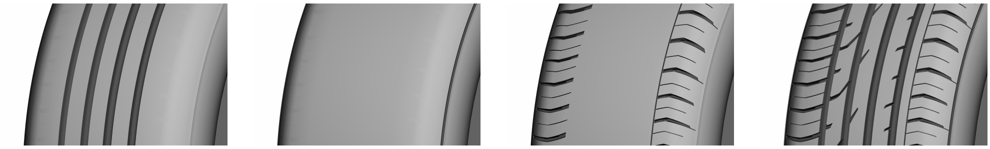

(a) *Main grooves* (b) *Side groove* (c) *Edge pattern* (d) *Full pattern*

Figure 2.2: *The three tyre features investigated and the full pattern they originate from*

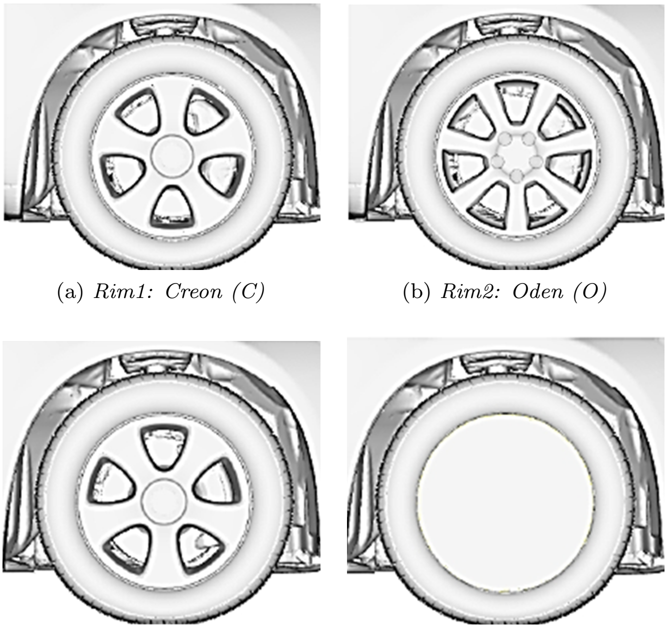

(a) *Rim1: Creon (C)* (b) *Rim2: Oden (O)*

(c) *Rim3: Creon Rotated (CR)* (d) *Rim4: Flat (F)*

Figure 2.3: *The four rims investigated*

One of the features which has been closely considered is referred to as Main Grooves, also known as rain grooves, which allow the evacuation of water from the tyre contact patch in order to prevent aqua planning and keep tyre grip with the road. These grooves can either be cut at the ground contact patch or they can be modified in ANSA so that it is still possible for airflow to pass through them. These two different methods of handling the main grooves at the contact patch are shown in fig. 2.4.

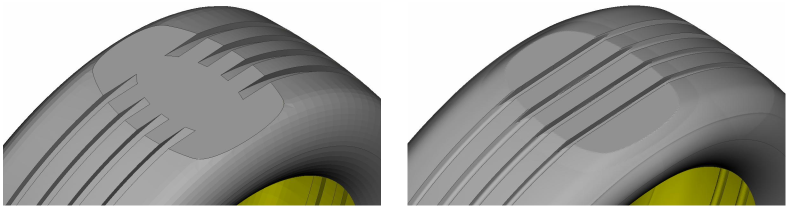

(a) *Main grooves cut* (b) *Main grooves connected*

Figure 2.4: *The two different ways of representing the main grooves at the contact patch seen from a bottom view*

The second set of simulations aimed at identifying the effects of the different methods available in CFD in order to simulate the rotation. For that purpose the Rotating Wall (RW) boundary condition, Moving Reference Frame (MRF), and Sliding Mesh (SM) methods have been investigated. In order to be able to have better control over the volume mesh generated around the wheels, they are placed in a separate cylindrical volume which is volume meshed using ANSA. A general mesh picture can be seen in fig. 2.5.

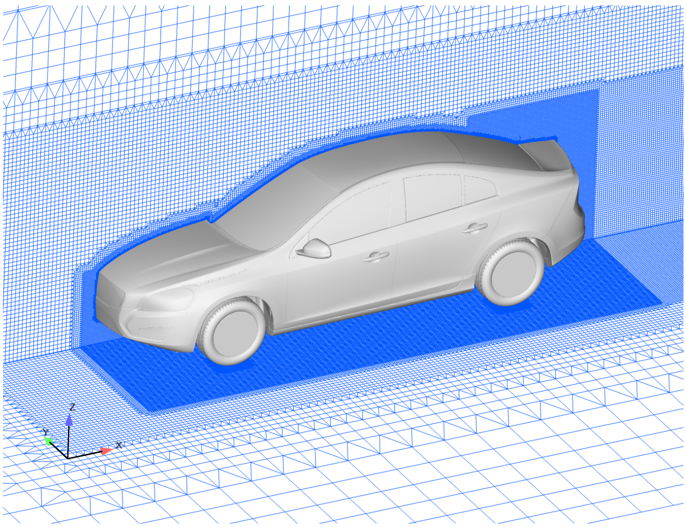

Figure 2.5: *Mesh visualization for closed front S60*

This cylindrical volume is rotationally symmetric as to allow it to rotate in the sliding mesh simulations. For that purpose the vehicle is floating 10 mm above ground level with the tyres undeformed and with no contact patch. Also as the computational expense for sliding mesh is significantly high, only a half car simulation could be performed thus reducing the number of sliding mesh volumes. This adds some inaccuracy to the overall forces acting on the vehicle during transient simulations however the purpose of this investigation is still to study the different effects of the rotation simulation methods. The RW method is known to be able to apply surface velocities at a tangent to the surface however when the desired velocity is perpendicular to the surface, the velocity vector is projected down, and the tangential component is applied. This leads to having almost zero velocity at the internal surfaces of the tyre pattern. On the other hand applying MRF on a cell in contact with that surface will result in the desired velocity magnitude and direction on the surface. This will also add some rotation into the flow as can be seen in fig. 2.6 when rotation is applied on a bar and the flow is visualized in a clip plane.

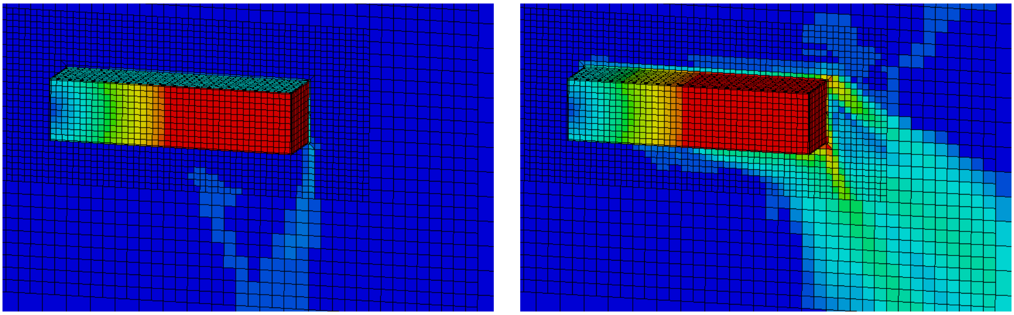

(a) *RW boundary condition* (b) *MRF on 1st volume cell*

Figure 2.6: *Velocity distribution on a bar and in the fluid for two different methods of applying rotation in steady state CFD simulations*

However, MRF also induces a pressure gradient into the flow field which in most cases is an undesirable effect. This pressure gradient is a numerical error introduced in cases where the flow is not aligned with the axis of rotation, which is usually the case a few millimeters away from the rims as the flow is dominated by the free stream and is aligned along the car. In such cases the volume of choice for MRF application can be quite crucial in introducing significant gradients which would affect the overall vehicle forces. In fig. 2.7 an empty disc with the respective size of a wheel is placed in a flow field with respective velocities to vehicle aerodynamics testing speeds. The MRF approach introduces a pressure gradient which slows down the flow on one part of the disc and accelerates it at the top part by more than 30% of the average free stream velocity at the peaks. In fig. 2.7 one can also see that for a SM approach this gradient is not introduced although small alteration of the flow field can still be seen.

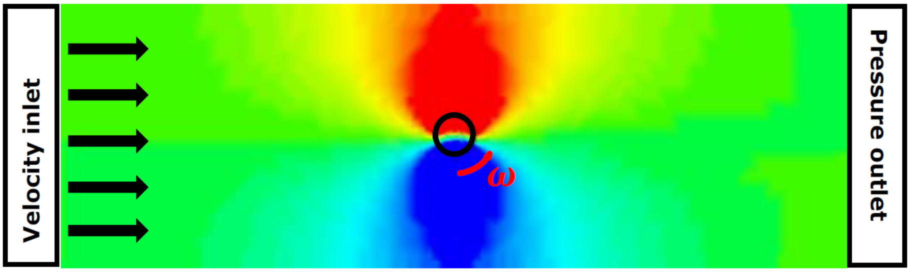

(a) *MRF on empty disc*

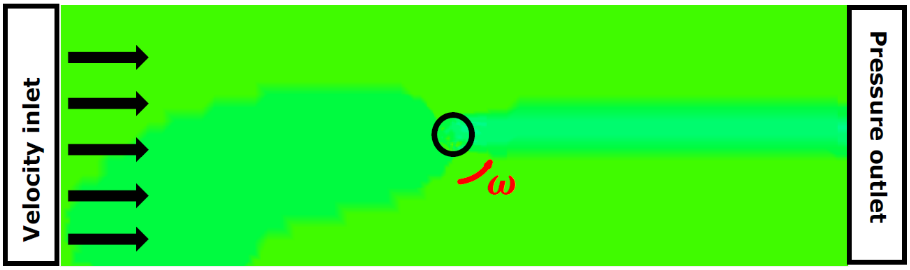

(b) *SM on empty disc*

Figure 2.7: *Velocity distribution in a fluid clip plane where two different methods are used to apply rotation on an empty cylindrical volume*

For this purpose a new approach to improve steady state simulations is suggested which combines both MRF and RW advantages. This approach, referred to as MRFG, utilizes RW to apply the rotation on the surface cells where tangential velocities are dominating and it utilizes MRF approach on the first volume cell for all other surfaces, which in this case are located inside the tyre pattern. The surfaces where MRF is implemented can be seen in fig. 2.8 and they are colored in dark purple and in addition fig. 2.9 shows the MRF volume cells highlighted in red.

(a) *Tyre 0 (T0) or Slick* (b) *Tyre 1 (T1)* (c) *Tyre 2 (2)*

Figure 2.8: *The three tyres that were used in rotation modelling investigations*

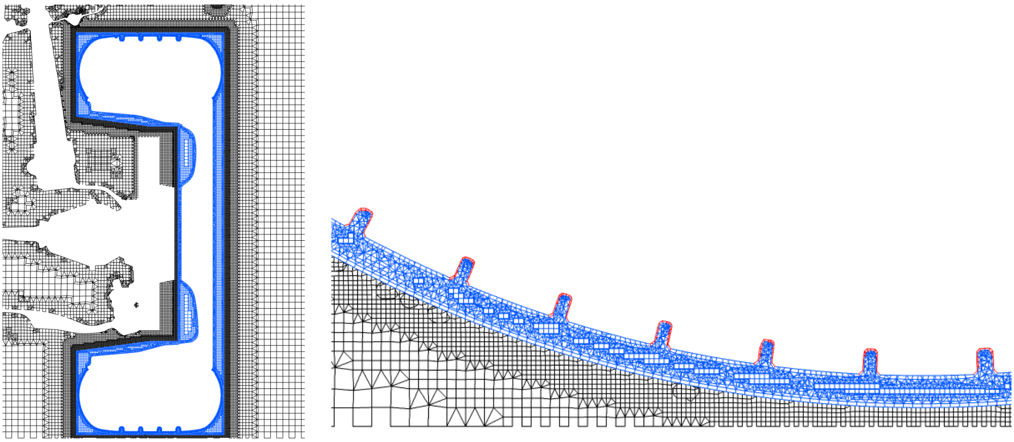

(a) *Mesh clip plane through front wheel center* (b) *Mesh clip plane highlighting in red the MRF application for MRFG*

Figure 2.9: *Mesh clip planes around the tyre. The blue volume mesh highlights the SM volume of rotation.*

2.2 Experimental Setup

The experiments aimed at measuring the air mass flow rate through a vehicle radiator using two different methods. The first method is a traditional one which is commonly used in vehicle aerodynamics applications. The second method is a novel approach developed by the author.
The pressure based method relies on placing several pressure probes across the radiator core. The probes are similar to a Prandtl tube where the output from each is a total pressure and a static pressure at the measurement point. Using this information the dynamic pressure can be computed and thus the the local velocity through the pressure probe is obtained. However as the geometry of the probe is not similar to the geometry of the radiator fins, this local probe velocity needs to be corrected. For that purpose, a calibration test needs to be performed in a test rig as a uniform flow through the radiator can be obtained and measured externally by the rig's measurement system. Each pressure probe is calibrated separately to the average velocity across the radiator core. When test measurements are performed, each probe measurement is corrected differently using its own calibration curve, then these local measurements are used to interpolate/extrapolate over the rest of the radiator core resulting in a velocity distribution. By integrating this distribution the volumetric flow rate is determined.
A DTC Initium data acquisition pressure system has been used for pressure measurements in the test rig. Two 32 port ESP scanners are used thus giving a total of 64 pressure measurements. As there are 48 probes in the radiator, a total of 96 pressure measurements need to be performed to get the capture the flow over the whole radiator. For that reason all tests in the rig where performed twice with one of the blocks alternating on different probes while the other maintains a fixed position for monitoring repeatability. The probes used for the measurements are the Ruijsink micro probes [28] which are shown in fig. 2.10 along with the pressure system used.

(a) *DTC Initium data aqusition unit* (b) *ESP pressure scanner* (c) *Ruijsink micro probes*

Figure 2.10: *Measurement equipment used in the test rig*

The calibration test has been performed at the Volvo GTT Fan Test Rig facility where the pressure drop vs. volumetric flow rate of the radiator has been empirically obtained. The test rig a closed loop plenum to plenum test rig, with the outlet chamber maintained at atmospheric pressure. The pressure drop is measured plenum to plenum and the air mass flow is measured by 6 venturi type nozzles (ISA 1932). Combinations of open and closed nozzles are used for different target mass flows in order to operate the nozzles within their correct Reynolds number range. More detailed information on the rig is available in Gullberg [33]. A schematic of the rig is shown in fig. 2.11 while the radiator setup is shown in fig. 2.12.

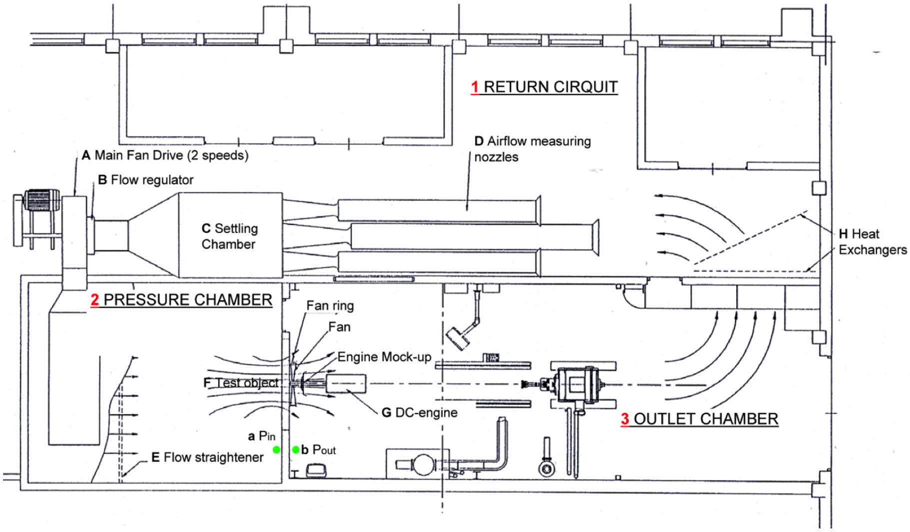

Figure 2.11: *Schematic fan test rig*

(a) *radiator set up in the pressure chamber* (b) *outlet chamber*

Figure 2.12: *Measurement equipment used in the test rig*

The force based method relies on measuring the force acting on the radiator core and then calculating the velocity through the radiator. In order to do that the pressure drop vs. volumetric air flow rate curve needs to be empirically extracted in the fan test rig. This curve can be converted into a force vs average velocity as the force is a result of the pressure drop integrated over the core area and the volumetric air flow rate is a result of the velocity integrated over the same core area. One can also notice that volumetric flow rate, mass flow rate and average core velocity are interchangeable terms with only constants separating them, following the 1-D equation of continuity presented in eq. 2.1.

$$\dot{m}_{core} = \dot{V}_{core} \times \rho_{air} = v_{average} \times A_{core} \times \rho_{air} \tag{2.1}$$

The wind tunnel facility used for this investigation is the Volvo Aerodynamic Wind Tunnel available at Volvo Cars, shown in fig. 2.13. It is a closed loop wind tunnel powered by a 5MW fan achieving speeds up to 250 km/h in the 27 m^2 test section. The tunnel delivers a free stream with turbulence intensity below 0.1 % and less than 0.6 degrees deviation from main flow direction [34]. The pressure system used at the wind tunnel is a PSI 8400 system with PSI ESP miniature electronic pressure scanners.

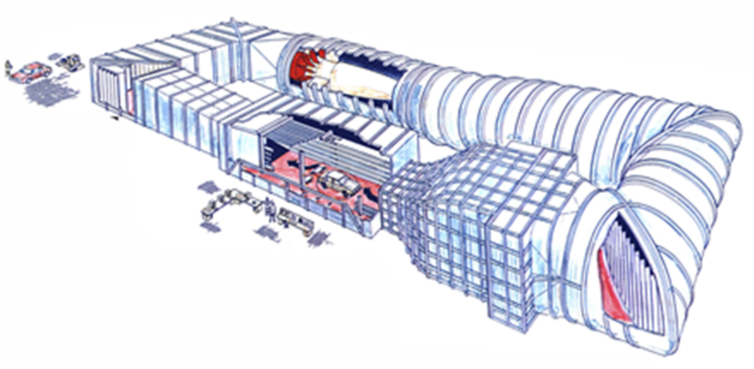

Figure 2.13: *Volvo Cars Aerodynamic Wind Tunnel*

The vehicle used in the test is a Volvo S60 production car. However for the purpose of this investigation some modifications had to be performed to the engine bay. For validation purposes, only one radiator is placed inside the vehicle as to have only one pressure drop. The radiator was suspended on load cells which attached the water tanks to the vehicle chassis. All components between the radiator and the front bumper were removed. All components connected to the radiator water tanks were removed except for the fan shroud which instead was mounted to the vehicle chassis. The fan was removed from the shroud. Also custom made aluminum ducts sealed the grill and spoiler inlets from the bumper to the radiator core, thus shielding out the water tanks. This allows the load cells to measure the force acting on the radiator core with minor influence from forces on the water tanks. Fig. 2.14 shows the radiator mountings on both sides of the water tanks connected to the chassis while fig. 2.15 shows the Reference configuration with the aluminum ducts sealing the bumper to the core.
Different grill configurations have been tested in the tunnel to demonstrate the usability of the new method and compare it to probe measurements. The spoiler opening, in the lower part of the front bumper, has been left completely open for all tests, as shown in fig. 2.15. The aim of the test is to vary inlet blockage in order to evaluate the method's ability to predict the mass flow with different flow distributions. The Reference configuration is the

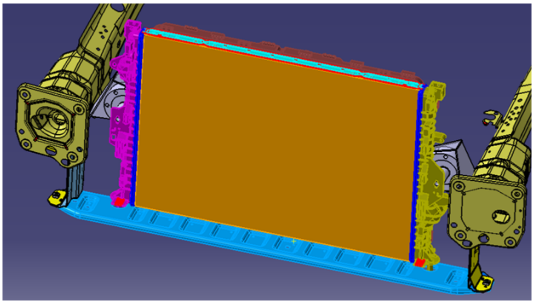

Figure 2.14: *Radiator mounting on load cells*

Figure 2.15: *Reference configuration showing the aluminum ducts*

minimum blockage configuration after which blockage starts increasing with Grill 1, 2, and 3 until reaching a Closed Grill. A realistic grill has been also tested for benchmarking purposes. The configurations investigated are shown in fig. 2.16 in order of increasing blockage (top to bottom, left to right).
For each configuration measurements where performed as continuous sweeps of increasing velocity from 80km/h to 200 km/h in increments of 20km/h to analyze the effects of velocity variations.

(a) *Grill 1: Open grill* (b) *Grill 2: Production grill* (c) *Grill 3*

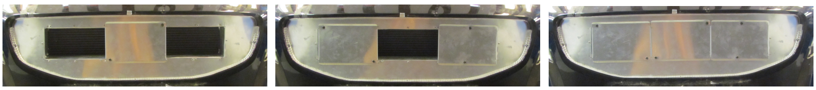

(d) *Grill 4* (e) *Grill 5* (f) *Grill 6: Closed grill*

Figure 2.16: *The different grill designs sorted by blockage ratio from completely open to completely closed*

3 Results and Discussions

3.1 Tyre Aerodynamics

3.1.1 Tyre Geometry Effect

Rain Grooves Some of the most largest features seen on tyres are rain grooves, large grooves that stretch around the circumference of the tyre Their main role is to allow water to pass under while the tyre keeps its contact patch. It has shown that accurate representation of the grooves at the contact patch is quite important as groove discontinuity at ground level gave opposite trends to actually connecting them. The grooves connect the high pressure zone in front of the wheels with the low pressure zone behind it as seen in fig. 3.1.

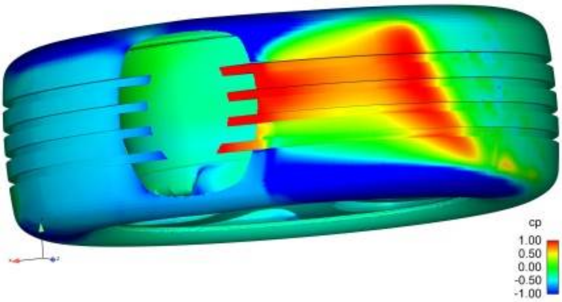

(a) *Cut rain grooves*

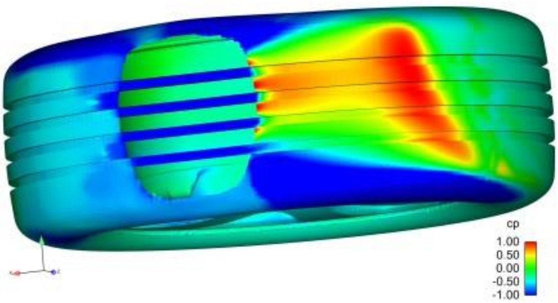

(b) *Connected rain grooves*

Figure 3.1: *Pressure distribution on the front left tyre from a bottom view*

This leads to a reduction in both the overall drag and lift of the vehicle, instead of an increase in both when the grooves are cut, which can be seen in fig. 3.2.

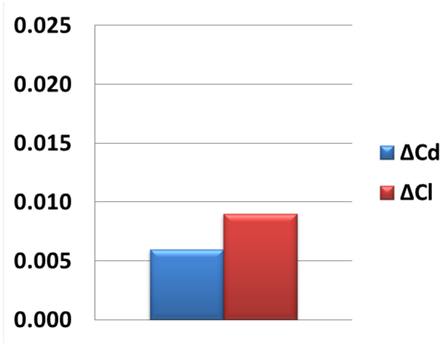

(a) *Cut rain grooves*

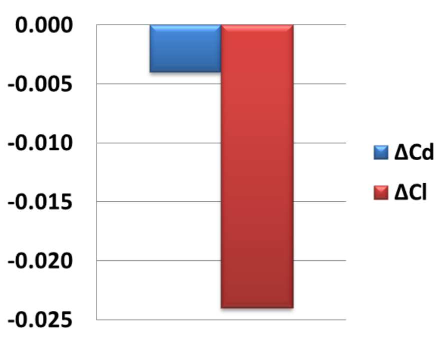

(b) *Connected rain grooves*

Figure 3.2: *Changes in C_d and C_l of the vehicle for the different rain grooves configuration referenced to a slick tyre*

In order to further investigate the effect of the connected grooves, main grooves have been added on different wheel geometries. This allowed to check for their consistent reductions in drag and lift of the overall vehicle on 16 different tyre/rim combinations. The results are presented in fig. 3.3

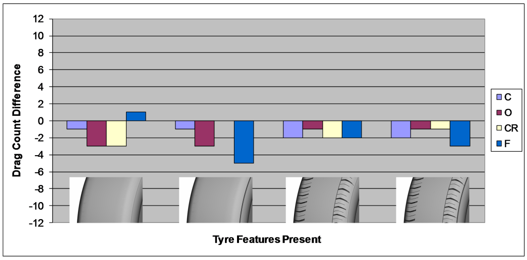

(a) *Overall C_d change*

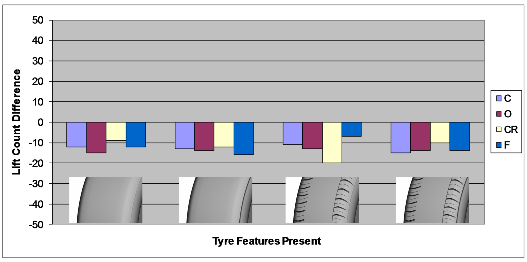

(b) *Overall C_l change*

Figure 3.3: *Overall change in vehicle aerodynamic coefficients when main grooves is added on different tyres and different rims*

Side Groove One Feature on the tyre which has a large effect on the overall vehicle forces in comparison to its small size is the side groove, which is the groove separating the pattern from the side wall of the tyre seen in fig. 2.2. This groove is quite small yet it falls in an area where the flow accelerates around the tyre's curved shoulder thus the flow is very susceptible to separation. When the flow reaches this rather small 3 mm deep and 5 mm wide gap a separation is triggered, as shown in fig. 3.4, which tends to increase drag and lift in most cases as presented in fig. 3.5. For the case of a flat rim where there is no interaction between with flow exiting the rim, this side groove actually reduced the overall drag of the vehicle.

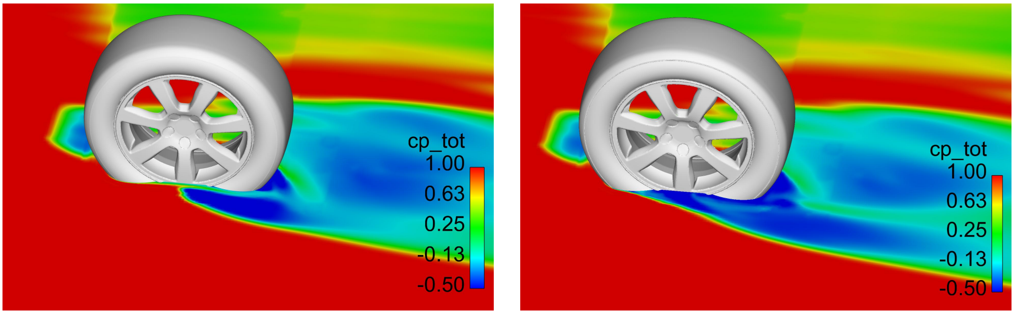

(a) *Without side groove* (b) *With side groove*

Figure 3.4: *Pressure distribution in a plane cut at the bottom of the rim showing the effect of adding a side groove on a slick tyre*

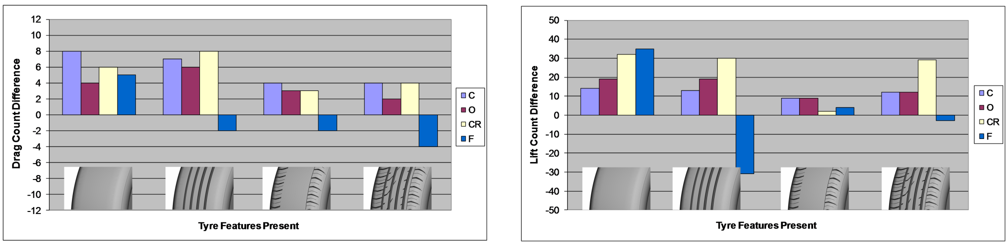

(a) *Overall C_d change* (b) *Overall C_l change*

Figure 3.5: *Overall change in vehicle aerodynamic coefficients when side groove is added on different tyres and different rims*

Full Pattern Different tyre patterns have also been investigated with clear differences showing on different parts of the vehicle. The two tyres are both the same size, from the same tyre manufacturer, and have the same general profile. The largest difference though was the pattern design itself, especially on the shoulder of the tyre. Although some of the most obvious differences in the flow field where seen in separations around the front wheels, the base separation was also affected with change in base pressure. The pressure distribution on the trunk of the car reflects the drag difference between the two as shown in fig. 3.6. Tyre 1 has shown an increase of 9 counts in drag and 10 counts in lift over Tyre 2.

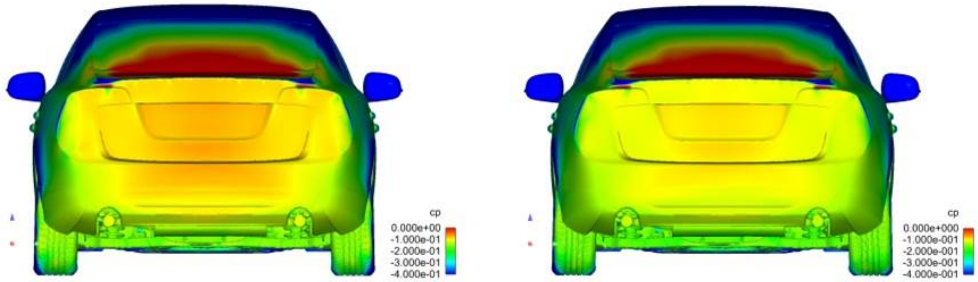

(a) *Tyre 1* (b) *Tyre 2*

Figure 3.6: *Pressure distribution on the base of the vehicle with two different tyre patterns*

In a comparison between the detailed tyres and the same tyres with rain grooves, significant increases in drag can be seen. Starting from a slick tyre the rain grooves lead to slight reductions in both drag and lift. As the detailed tyres are more geometrically similar to grooved tyres then it is more relevant to compare them to these instead. The results from such a comparison are summarized in fig. 3.7 showing significant increase in drag and lift on different rims. This shows a strong dependency on rim design. Although in the results showed below tyre 2 was consistent in giving lower drag and lift increase, sometimes the difference was marginal. This shows that for a certain rim design, tyre 2 could result in higher drag than tyre 1 or at least one would not see any aerodynamic difference between the two tyres.

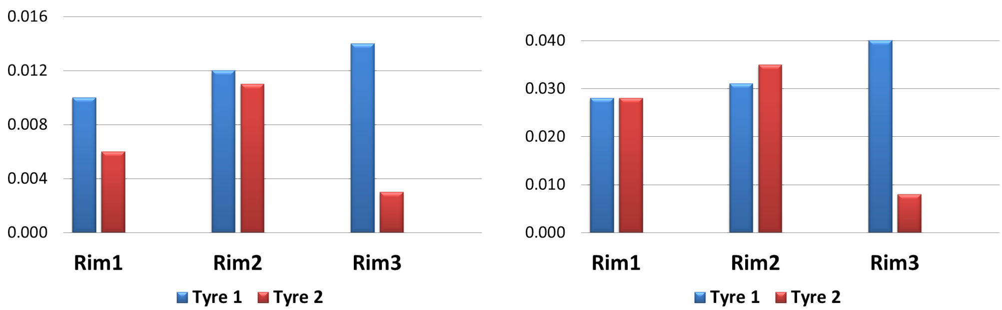

(a) *Delta C_d* (b) *Delta C_l*

Figure 3.7: *Changes in vehicle aerodynamic coefficients when adding different tyre patterns on different rims in reference to a slick tyre*

3.2 Tyre Rotation Modelling Effect

Full Pattern Modelling Apart from the tyre rim dependency when full pattern tyres are meshed for CFD computations, the method of modelling the tyre rotation can also have a significant effect on the results. This is shown when RW, MRF, MRFG, and SM are used to simulate the rotation of tyres T1 and T2 on a closed rim. The changes in C_d and C_l of the overall vehicle are presented in the fig. 3.8 with the slick tyre as reference.

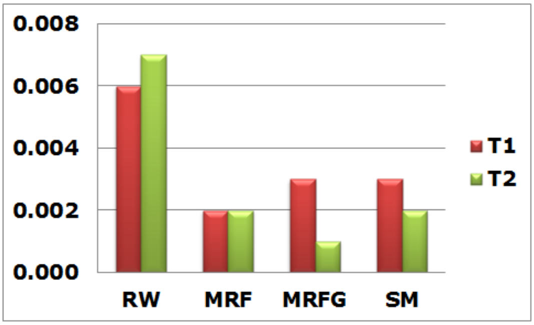

(a) *Delta C_d*

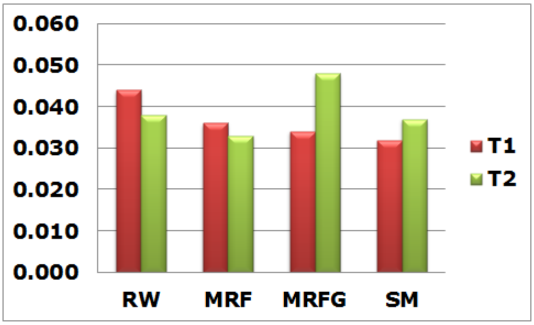

(b) *Delta C_l*

Figure 3.8: *Changes in Cd and Cl of the vehicle when using different modelling methods for tyre rotation on a closed rim and referenced to T0*

Note that these results are preformed on a different vehicle geometry and placed in a different flow field, thus they are not directly comparable to the previous mentioned results yet they still shed some light on the importance of modelling investigations. One must also note that since these simulations are performed with a closed flat rim, there is no outflow from the rim thus the results from the sliding mesh simulations are considered to be mainly due to sliding the tyres and not the rim.
It can be seen that the RW method tends to over predict the increase in drag when tyre pattern details are added in comparison to the other methods. on the other hand when MRFG is implemented it has a significant effect on the flow field even though it only effects few cells located inside the tyre pattern. MRFG also shows potential in predicting

the trends of the drag increase of the different tyres even though it still over predicted the lift for T2 when comparing to SM. However, with lack of experimental data it is not possible to analyze in comparison with real life tests, so SM is in this case considered to be the most realistic of the used modelling methods as it consists of physical mesh rotation, even though this remains to be investigated. Another important result is that the MRFG can be implemented in steady state simulations thus significantly reducing the computational hours needed for the simulation. A comparison of cluster time required for each simulation is presented in fig. 3.9, and shows that the SM approach is 25 times more costly than RW, MRF, and MRFG which all need the same number of hours.

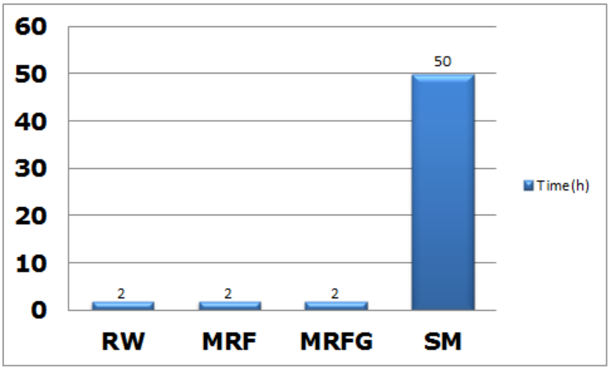

Figure 3.9: *Solving time in hours required on 512 cores on cluster*

3.3 Cooling Flow

This section includes results from the fan test rig as well as the wind tunnel, separated in two different sections. The results obtained in the fan test rig are used to be able to calculate the mass flow through the radiator after in has been placed in the S60 test car the wind tunnel.

3.3.1 Fan test rig results

The main aim of using the fan test rig is to calibrate the pressure probes, and extract the property curves of the radiator used later to calculate the mass flow from the force measurements.

Pressure probe calibration Calibrating the pressure probes is needed as the geometry of the probes is not representative to the geometry inside the radiator core. This results in different blockage at the point where the probes are mounted and thus resulting in a different flow velocity through the probe than the radiator fins around it. Also the probes are mounted manually, and although one can try to apply the same method for all the probes, some probes will end up being a bit tilted and or will block different fins. Also the radiator fins are so delicate that they will twist differently for each probe. This means that a separate calibration curve needs to be computed for each probe, and as shown in fig. 3.10, 48 calibration curves for the 48 probes mounted in the radiator are presented.

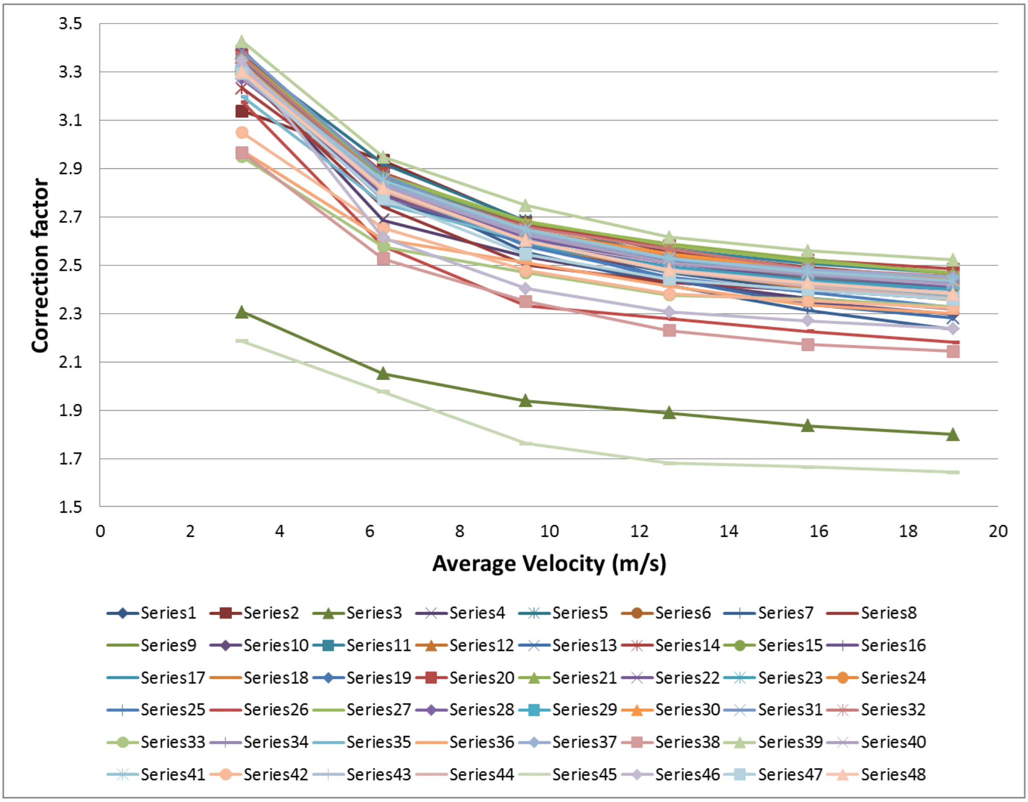

Figure 3.10: *Calibration curves for the 48 pressure probes*

After the calibration curves are obtained, a quick test is performed in order to ensure that the measured valued correspond the overall mass flow this method aims at measuring. This allows also to check for the accuracy of the method for a few configurations. Thus a fan shroud is mounted on the leeward side of the radiator at a similar distance from the radiator core as in the wind tunnel test. This allows to create an inhomogeneous velocity distribution on the radiator core so the measurements could be checked for a complex flow scenario. Both the shroud setup and the flow distribution across the core can be seen in fig. 3.11. The results show that the measured accuracy for 5 different mass flows was within $\pm$ 2% uncertainty, yet one should note that the inhomogeneity was relatively low, below 20%.

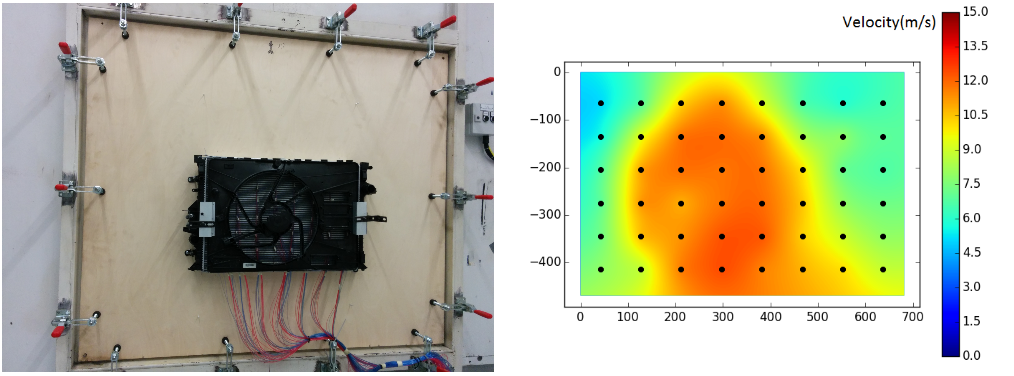

(a) *Shroud setup* (b) *Velocity distribution on radiator*

Figure 3.11: *Fan shroud configuration in the test rig to check calibration and accuracy of the probe system*

3.3.2 Wind tunnel results

The following sections demonstrate the force based approach's ability to measure the air mass flow. Paragraph "Initial results" presents the results in their most basic form without any corrections. Paragraph "Force distribution correction" will compare the force-predicted velocity to its theoretical equivalent obtained from analyzing the velocity distribution from the pressure based approach. Paragraph "Center of pressure correction" shows that the force based approach can be a standalone method for predicting the mass flow by applying a correction to the over predicted velocities based on the center of pressure position on the radiator. Finally, "Uncertainty" discusses the different uncertainties between a global force based approach compared to local traditional approaches.

Initial Results The results presented in this section are the percentage difference between the average velocities predicted by the load cells v_{avg_F} compared to that predicted by the probes v_{avg_P}. As can be seen in fig. 3.12, the force measurement shows in most cases an over prediction of the velocity predicted by the probes. One can notice from the graph above that for grills with low blockage, like grills 1, 2, and 3, the mass flows predicted by the force is already within the measurement uncertainty of the pressure probes. However as the blockage increases the over prediction increases as shown for Grills 4, 5, and 6. This is mainly due to the increase in flow inhomogeneity through the radiator. This can be visualized by plotting the velocity distribution through the radiator for the different configurations with the inhomogeneity value for each respective grill configuration at a testing velocity of 200 km/h as shown in fig. 3.13. The equation for calculating inhomogeneity used in this paper is taken from Hucho [35] and presented in eq. 3.1.

$$i = \frac{1}{n}\sum_{k=1}^{n}\frac{\left|\dot{m}_K\frac{A_R}{A_K} - \dot{m}_{tot}\right|}{\dot{m}_{tot}} \qquad (3.1)$$

where n is the number of measurement points, $\dot{m}_K$ is the mass flow through one area section, A_K is the size of one area section, A_R is the size of the radiator core area, and $\dot{m}_{tot}$ is the total mass flow through the radiator.

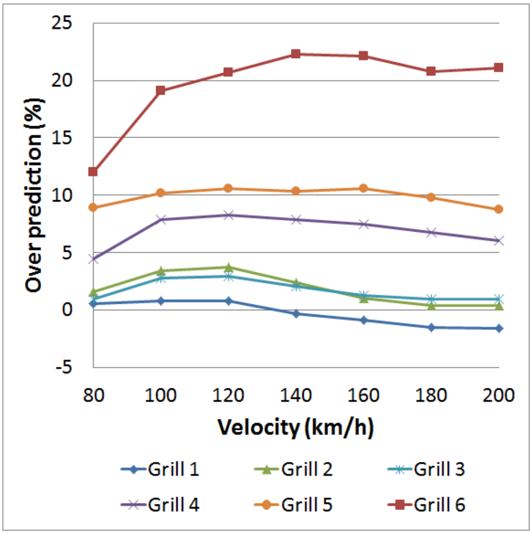

Figure 3.12: *Percentage over prediction comparing v_{avg_F} to v_{avg_P}*

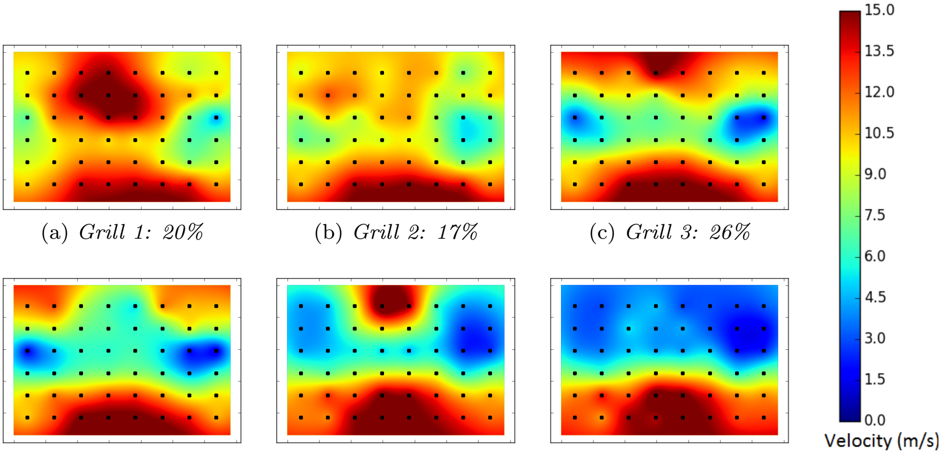

(a) *Grill 1: 20%* (b) *Grill 2: 17%* (c) *Grill 3: 26%*

(d) *Grill 4: 32%* (e) *Grill 5: 40%* (f) *Grill 6: 55%*

Figure 3.13: *Velocity distribution through the radiator core for the different grill configurations at 200km/h testing speed. Inhomogeneity values are also presented beneath each plot, respectively*

Force distribution correction The main challenge in predicting mass flow comes from the relation between the force and mass flow which is not linear but rather described by a second order polynomial. As a result the average force acting on the radiator will always over predict the average velocity through it. This over prediction needs to be corrected for, thus introducing some uncertainties. An example of this over prediction is shown in fig. 3.14, where the color yellow depicts two velocity measurement points. The green line represents the results if one would look at the velocity average. The purple lines represent the results if one would look at the force average. As observed, the average velocities using the different approaches do not match. The force averaging causes an over prediction of 0.5 m/s in average core velocity. This is equivalent to a 4 % over prediction of the mass flow. Knowing that the force will in theory over predict the real mass flow, it

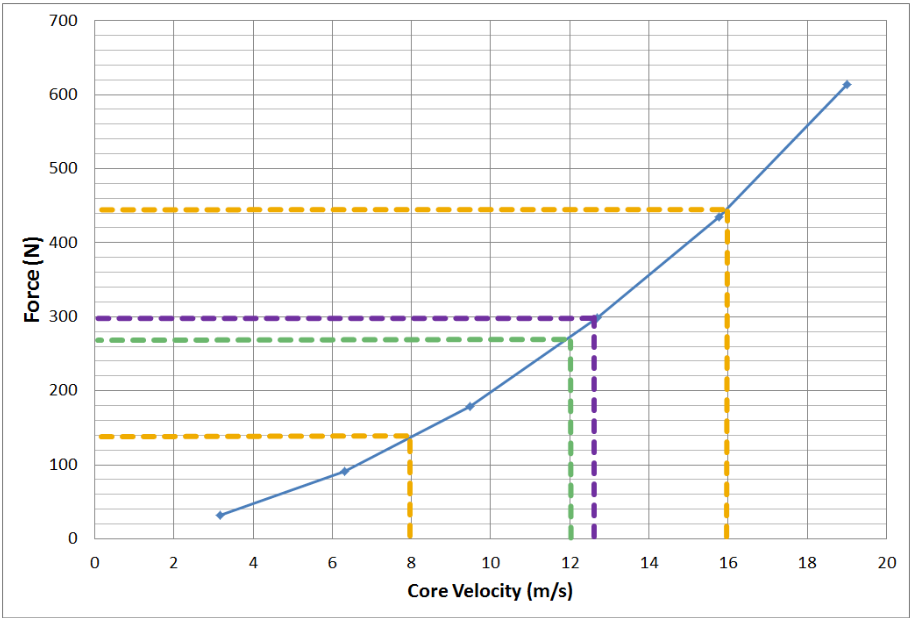

Figure 3.14: *Over prediction demonstration on force versus velocity curve*

is not possible to validate the reliability of the test setup by comparing raw results to the average velocity predicted by the pressure probes. For that reason, a force distribution can be calculated from the pressure probes measurements. Thus the total force F_{Tot} acting on the radiator can be calculated with the distribution taken into account. Due to the fact that the quantity of interest is the mass flow, one could calculate an over predicted velocity v_{avg_Theory}. Comparing percentage difference between v_{avg_F} and v_{avg_Theory} can be seen in fig. 3.15. This allows one to check whether the current test setup is able to measure the over predicted mass flow.
Except for the closed grill configuration, velocity predicted by the forces falls within the ± 5 % uncertainty of the probe predictions. This brings confidence that the setup used to measure the force acting on the radiator is working as expected. This also proves that

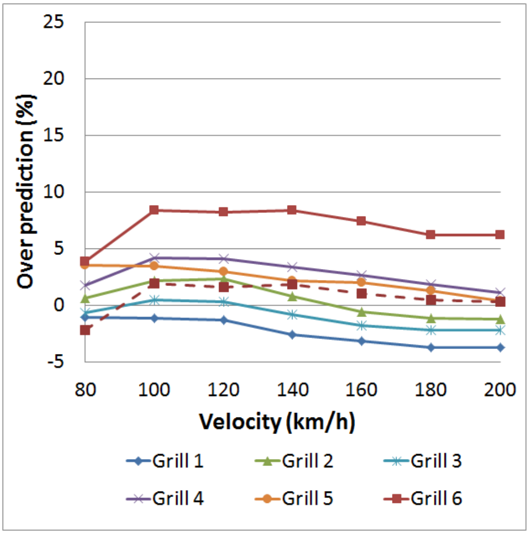

Figure 3.15: *Percentage over prediction comparing* v_{avg_F} *to* v_{avg_Theory}

the force distribution on the radiator is the most significant uncertainty in predicting flow rate from a force measurement.
Concerning the closed cooling curve which still did not fall within the assumed ± 5 % margin, an investigation into the discretization has been carried out. This is performed in order to check how accurately the current grid could capture the flow distribution, when inhomogeneity figures as high as 55% are measured. For that purpose a quick check on the steep transition between rows 4 and 5 of the probes is carried out. Although the transition looks smooth in the figure, that is only due to the linear interpolation over a fine grid for the purpose of integrating over the radiator. In reality, this transition could be quite abrupt and could happen anywhere between rows 4 and 5. The effects of having an abrupt transition at row 4 versus one at row 5 yields a 13 % difference in flow rate through the radiator. Doing the same for a radiator with homogeneous flow such as Realistic Grill or Reference configuration yields less than 2 % difference. Due to the high gradient influence and for the fact that the pressure probe's reliability at measuring the low velocities covering more than half of the radiator is questionable given fig. 3.10, a suggested correction for the transition effect of the Closed Grill is shown in fig. 3.15 as a dotted line, which now fits with the other tested configurations.

Center of Pressure Correction After having shown that the force method application matches theory, and demonstrating how it over predicts the flow rate, a correction needs to be performed and it is based on the center of pressure position. In the current test setup, the center of pressure cannot be located through the load cells measurements since there are only two of them. However, center of pressure can be calculated from the force distribution in order to investigate the possibilities it could offer. In another test setup where one would use four load cells, the center of pressure could be calculated from the force measurements. In this test the over prediction expected due to the force distribution can be calculated from v_{avg_Theory} to v_{avg_P} ratio. By calculating the center of pressure distance to the radiator center one could plot the over prediction versus the distance for the whole set of measurements. As shown in fig. 3.16 the set of data seem to describe a second order degree polynomial. Such a curve could also be extracted from a fan test rig when it is possible to measure forces acting on the radiator core in the fan test rig. The complete set of measurements, including all grill configurations and yaw angle simulations, is used to obtain the plot in fig. 3.16 . So the best fit curve is a universal curve of correction which is not case dependent as for the force distribution case. It is worth noting however that for low offsets and corrections below 5% the curve fitting is not ideal as the changes are so small they fall within the uncertainty of the measurements.

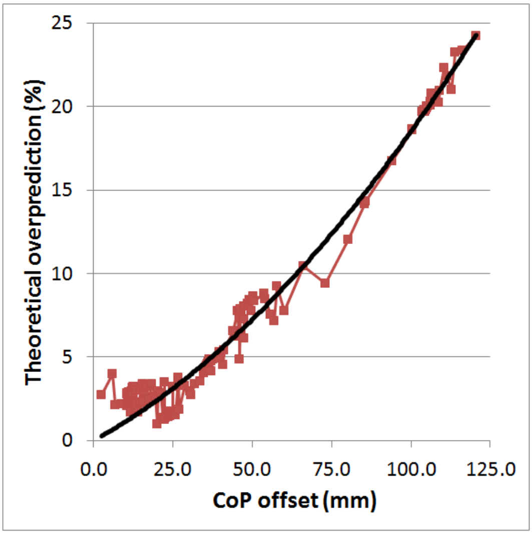

Figure 3.16: *Percentage over prediction comparing v_{avg_Theory} to v_{avg_P} plotted against CoP offset from the geometric center of the radiator. The curve fit represents the CoP correction curve.*

By using the correction curve presented in fig. 3.16, the raw results of the over prediction can be corrected. Fig. 3.17 shows the corrected results, with the corrected set of data clearly between a $\pm$ 5 % uncertainty margin. In extreme cases, high inhomogeneity does not necessarily cause a large shifting of the center of pressure from the center of the radiator. However a significant shift in the center of pressure can only be due to high inhomogeneity. As seen in fig. 3.18, when CoP distance to geometric center of the core is quite significant, as in the Closed Grill configuration this gives a large correction that accounts for the large inhomogeneity. However for cases where the shift in inhomogeneity and CoP are not that large, then the correction would only have little effect of about 1 to 2 % in the cases of Grill 1 and 2 for example.

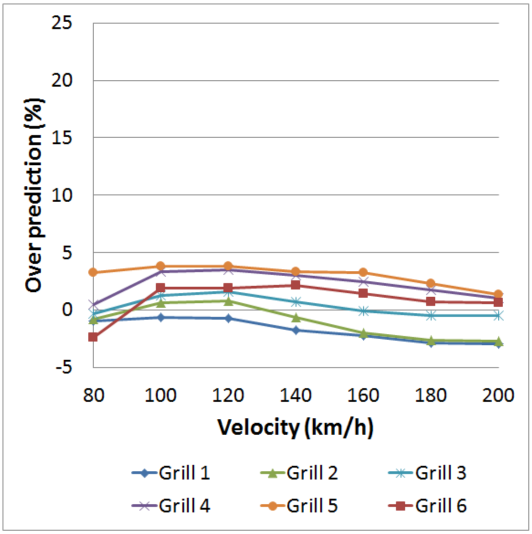

Figure 3.17: *Percentage over prediction comparing v_{avg_Corr} to v_{avg_P}*

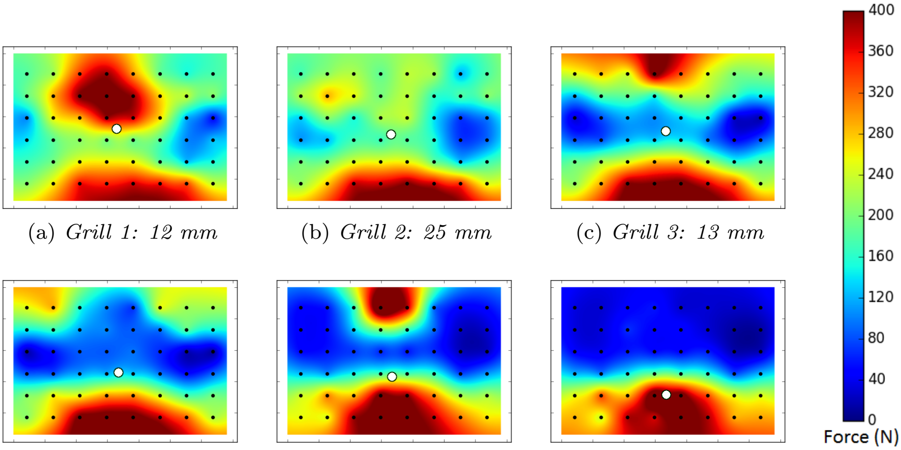

(a) *Grill 1: 12 mm* (b) *Grill 2: 25 mm* (c) *Grill 3: 13 mm*

(d) *Grill 4: 37 mm* (e) *Grill 5: 50 mm* (f) *Grill 6: 107 mm*

Figure 3.18: *Force distribution over the radiator core for the different grill configurations at 200km/h testing speed. The CoP is presented as the larger white dot on each plot with the offset value from geometrical center written beneath*

Uncertainty Both of the traditional approaches described in the "Introduction" require several measurement points across the radiator core, which then need to be integrated over the total core area to compute the mass flow. This risks adding additional blockage in the flow field by the measurement equipment. Kuthada [36] also shows through a CFD simulation investigation that for an averaged vehicle size radiator with about 19 % inhomogeneity, around 50 probe measurements are recommended to be able to predict the within a 2.5 % error margin only due to discretization error. For a given radiator size, a certain measurement grid density needs to be considered to achieve high accuracy. However as shown in "Discretization correction" section, this error can increase significantly to higher than 10 % with an increase in inhomogeneity. The overall accuracy of the micro probes have shown to be within 2.2 % error margin in the test rig when blockage behind the radiator is added to increase the inhomogeneity to 23 %. Similar results are reported by Kuthada [37].

The force approach does not suffer from the uncertainty introduced by discretization which itself is dependent on measurement grid density across the radiator core. However it does introduce uncertainty as it over predicts the mass flow due to force distribution. This can be corrected for using information of the center of pressure position. Initial results show that predicted mass flow is within a $\pm$ 5 % error margin compared to the pressure probes' prediction. This is considered acceptable as it lies within the overall uncertainty of the pressure based method.

4 Conclusion

4.1 Summary

The thesis presents a collection of works covering simulation of tyres in CFD and measurements of cooling flow through a radiator. An analysis of the tyre geometry effect is performed which highlights the effects of such relatively small geometrical details. A new method (MRFG) has also been suggested to better model the rotation of the tyres. Also, a new force based method for measuring air mass flows through radiator has been presented and compared to a traditional pressure based method.
From the work presented some conclusions can be made, most important of which are:

- Accurate representation of the tyre deformation at the contact patch has significant effects on drag and lift forces acting on the vehicle
- There is a strong interaction between the rim and tyre which makes it particularly hard to optimize each separately
- The method of rotation modelling of the tyre can significantly impact the drag and lift forces of the car
- When it comes to tyre pattern comparisons in CFD, advanced rotation modelling approaches, like MRFG, show promising results in capturing similar trends to SM at 4 % of the the cost
- The novel force based approach for measuring air flow rate through radiators showed promising results and comparable accuracy to a traditional pressure based approach, while offering numerous advantages and reliable data acquisition systems

4.2 Future Work

From the conclusions presented above a given that this work is part of a larger project with longer aim goals, a set of future work investigations can be suggested:

- Further investigations on tyre rotation modelling will be performed and the simulations will be compared to experimental data
- MRFG will be tested on detailed tyres with contact patches in order to investigate its influence in a more realistic test scenario
- CFD simulations will be performed on similar configurations to the wind tunnel tests in order to compare the prediction of air mass flow through the radiator
- A more thorough comparison between the pressure based method and force based method will be performed to get more accurate figures on the uncertainties of each in different flow conditions

References

[1] J. Fackarell and J. Harvey. *The Flow Field and Pressure Distribution of an Isolated Road Wheel*. Paper 10. Advances in Road Vehicle Aerodynamics, 1973.

[2] A. Cogotti. Aerodynamic characteristics of car wheels. *Int. Journal of Vehicle Design* (1983), pp. 173–196.

[3] L. Axon, K. Garry, and J. Howell. *An Evaluation of CFD for Modelling the Flow Around Stationary and Rotating Isolated Wheels*. Paper No: 980032. Warrendale and PA: SAE International, 1998. DOI: 10.4271/980032.

[4] E. Mercker et al. *On the Aerodynamic Interference Due to the Rolling Wheels of Passenger Cars*. Paper No: 910311. Warrendale and PA: SAE International, 1991.

[5] E. Mercker and H. Berneburg. "On the Simulation of Road Driving of a Passenger Car in a Wind Tunnel Using a Moving Belt and Rotating Wheels". *3rd Int. Conf. Innovation and Reliability*. Florence, April 8-10, 1992.

[6] E. Mercker, H. Soja, and J. Wiedemann. *Experimental investigations on the Influence of Various Ground Simulation Techniques on a Passenger Car*. Conference on Vehicle Aerodynamics. Proceedings Roy. Aer.Soc, 1994.

[7] M. Pfadenhauer, G. Wickern, and K. Zwicker. "On the Influence of Wheels and Tyres on the Aerodynamic Drag of Vehicles". *MIRA International Conference on Vehicle Aerodynamics*. 1996.

[8] G. Wickern. "The Effect of Moving Ground on the Aerodynamic Drag of a Production Car". *SATA Conference*. 1991.

[9] G. Wickern, K. Zwicker, and M. Pfadenhauer. *Rotating Wheels - Their Impact on Wind Tunnel Test Techniques and on Vehicle Drag Results*. Paper No: 970133. Warrendale and PA: SAE International, 1997.

[10] I. Dimitriou and S. Klussmann. *Aerodynamic Forces of Exposed and Enclosed Rotating Wheels as an Example of the Synergy in the Development of Racing and Passenger Cars*. Paper No: 2006-01-0805. Warrendale and PA: SAE International, 2006.

[11] P. Elofsson and M. Bannister. *Drag Reduction Mechanisms Due to Moving Ground and Wheel Rotation in Passenger Cars*. Paper No: 2002-01-0531. Warrendale and PA: SAE International, 2002.

[12] C. Landström, L. Löfdahl, and T. Walker. *Detailed Flow Studies in Close Proximity of Rotating Wheels on a Passenger Car*. Paper No: 2009-01-0778. Warrendale and PA: SAE International, 2009.

[13] C. Landström et al. "An experimental investigation of wheel design parameters with respect to aerodynamic drag". *8th FKFS Conference-Progress in Vehicle Aerodynamics and Thermal Management*. Stuttgart, 2011.

[14] C. Landström et al. *Influences of Different Front and Rear Wheel Designs on Aerodynamic Drag of a Sedan Type Passenger Car*. Paper No: 2011-01-0165. Warrendale and PA: SAE International, 2011.

[15] W. Mayer and J. Wiedemann. *The Influence of Rotating Wheels on Total Road Load*. Paper No: 2007-01-1047. Warrendale and PA: SAE International, 2007.

[16] J. McManus and X. Zhang. A Computational Study of the Flow Around an Isolated Wheel in Contact With the Ground. *Journal of Fluids Engineering* 128.3 (2006), p. 520. ISSN: 00982202.

[17] F. Modlinger, R. Demuth, and N. Adams. "New Directions in the Optimization of the Flow around Wheels and Wheel Arches". *MIRA International Conference on Vehicle Aerodynamics*. 2008.

[18] A. F. Skea, P. R. Bullen, and J. Qiao. *CFD Simulations and Experimental Measurements of the Flow Over a Rotating Wheel in a Wheel Arch*. Paper No: 2000-01-0487. Warrendale and PA: SAE International, 2000.

[19] A. Wäschle et al. *Flow around an Isolated Wheel - Experimental and Numerical Comparison of Two CFD Codes*. Paper No: 2004-01-0445. Warrendale and PA: SAE International, 2004. DOI: `\url{10.4271/2004-01-0445}`.

[20] A. Wäschle. *The Influence of Rotating Wheels on Vehicle Aerodynamics - Numerical and Experimental Investigations*. Paper No: 2004-01-0445. Warrendale and PA: SAE International, 2007. DOI: `\url{10.4271/2007-01-0107}`.

[21] P. Mlinaric and S. Sebben. "Investigation of the Influence of Tyre Deflection and Tyre Contact Patch on CFD Predictions of Aerodynamic Forces on a Passenger Car". *MIRA International Conference on Vehicle Aerodynamics*. 2008.

[22] F. Wittmeier et al. "Model Scale Based Process for the Development of Aerodynamic Tire Characteristics". *SAE Technical Paper*. SAE International, Apr. 2014. DOI: 10.4271/2014-01-0585.

[23] B. Schnepf, T. Schütz, and T. Indinger. Further Investigations on the Flow Around a Rotating, Isolated Wheel with Detailed Tread Pattern. *SAE Int. J. Passeng. Cars - Mech. Syst.* 8 (Apr. 2015), pp. 261–274. DOI: 10.4271/2015-01-1554.

[24] C. Landstrom et al. Aerodynamic Effects of Different Tire Models on a Sedan Type Passenger Car. *SAE Int. J. Passeng. Cars - Mech. Syst.* 5 (Apr. 2012), pp. 136–151. DOI: 10.4271/2012-01-0169.

[25] F Wittemeier et al. "Classification of Aerodynamic Tyre Characteristics". *International Vehicle Aerodynamics Conference 2014*. Holywell Park, Loughborough, UK, 2014, pp. 175–185. ISBN: 978-0-08-100199-8.

[26] B. Schnepf, G. Tesch, and T. Indinger. "Investigations on the Flow around Wheels using Different Road Simulation Tools". *Progress in Vehicle Aerodynamics and Thermal Management*. Stuttgart, Germany, 2013, pp. 155–166. ISBN: 978-3-8169-3253-6.

[27] E. Y. Ng et al. "Use of Pressure-Based Technique for Evaluating the Aerodynamics of Vehicle Cooling Systems". *SAE Technical Paper*. Detroit, Michigan: SAE International, 2002. DOI: 10.4271/2002-01-0712.

[28] R Ruijsink. "The Use of the MicroProbe System in Cooling System Development". *Third MIRA International Vehicle Aerodynamics Conference*. Rugby, UK, 2000. ISBN: 0952415623.

[29] S. Wille et al. Integrated Numerical and Experimental Approach to Determine the Cooling Air Mass Flow in Different Vehicle Development Stages. *SAE Int. J. Passeng. Cars - Mech. Syst.* 3 (1 2010), pp. 352–365. ISSN: 1946-4002. DOI: 10.4271/2010-01-0287.

[30] J. F. Foss et al. The Thermal Transient Anemometer. *Measurement Science and Technology* 15 (11 2004), pp. 2248–2255. DOI: 10.1088/0957-0233/15/11/010.
[31] J. Williams. "An Automotive Front-End Design Approach for Improved Aerodynamics and Cooling". *SAE Technical Paper*. Detroit, Michigan: SAE International, 1985. DOI: 10.4271/850281.
[32] J. Williams and G. Vemaganti. "CFD Quality - A Calibration Study for Front-End Cooling Airflow". *SAE Technical Paper*. Detroit, Michigan: SAE International, 1998. DOI: 10.4271/980039.
[33] P. V. Gullberg. "Optimisation of the Flow Process in Engine Bays- 3D Modelling of Cooling Airflow". PhD thesis. Gothenburg, Sweden, 2011, pp. 239–245. ISBN: 978-91-7385-559-4.
[34] J. Sterneus, T. Walker, and T. Bender. "Upgrade of the Volvo Cars Aerodynamic Wind Tunnel". *SAE Technical Paper*. Detroit, Michigan: SAE International, 2007. DOI: 10.4271/2007-01-1043.
[35] W. H. Hucho. *Aerodynamics of Road Vehicles*. Fourth. Warrendale, USA: Society of Automotive Engineers, Inc, 1998, pp. 559–561. ISBN: 0-7680-0029-7.
[36] T. Kuthada. A review of Some Cooling Air Flow Measurement Techniques for Model Scale, Full Scale and CFD. *SAE Int. J. Passeng. Cars - Mech. Syst.* 6 (1 2013), pp. 88–96. ISSN: 1946-4002. DOI: 10.4271/2013-01-0598.
[37] T. Kuthada. "Die Optimierung von Pkw Kühllüftungssystemen unter dem Einfluss moderner Bodensimulationstechniken". PhD thesis. Stuttgart, Germany, 2006, pp. 50–53. ISBN: 3-8169-2664-9.
[38] T. Hobeika, S. Sebben, and C. Landstrom. Investigation of the Influence of Tyre Geometry on the Aerodynamics of Passenger Cars. *SAE Int. J. Passeng. Cars - Mech. Syst.* 6 (1 2013), pp. 316–325. ISSN: 1946-4002. DOI: 10.4271/2013-01-0955.
[39] T. Hobeika, S. Sebben, and L. Lofdahl. "Study of Different Tyre Simulation Methods and Effects on Passenger Car Aerodynamics". *International Vehicle Aerodynamics Conference 2014*. Holywell Park, Loughborough, UK, 2014, pp. 187–195. ISBN: 978-0-08-100199-8.
[40] T. Hobeika, S. Sebben, and L. Lofdahl. A Novel Approach for Air Flow Rate Measurement Through Heat Exchangers. *Experiments in Fluids* (2015). submitted.
[41] T. Hobeika, A. Vdovin, and L. Lofdahl. "Influence of Rims and Tyres on the Aerodynamic Resistance of Passenger Vehicles". *Tagung Fahrzeugaerodynamik*. Munich, Germany, 2014.